Atomic Charges for Classical Simulations of Polar Systems

Hendrik Heinz* and Ulrich W. Suter

Department of Materials, Institute of Polymers, ETH Zurich, CH-8092 Zurich, Switzerland

Received: April 28, 2004; In Final Form: August 9, 2004

Structure and reactivity often are dependent on the polarity of chemical bonds. This relationship is reflected by atomic charges in classical (semiempirical) atomistic simulations; however, disagreement between atomic charges from accurate experimental investigations, ab initio methods, and semiempirical methods has not been resolved. Our aim is to improve the basic understanding of the polarity of compounds with a view to make force-field parametrizations more consistent and physically realistic. The concept is based on the relationship between the atomization energies of the elements and the possible strength of covalent bonding and the relationship between the ionization energies/electron affinities of the elements and the possible strength of ionic bonding. Both quantities, energetically, are of the same order of magnitude and influence atomic charges in a compound, which we illustrate by trends across the periodic table. The relationship between the pure elements and a given compound is shown in an extended Born model. We note that the extended Born model can be used to obtain physically justified charge estimates, relative to available reference compounds. This semiempirical concept has a stronger foundation than electronegativity equalization [Rappe, A. K.; Goddard, W. A., III. *J. Phys. Chem.* **1991**, *95*, 3358−3363], which is based on isolated gas-phase atoms and does not include covalent bonding contributions. We demonstrate the assignment of atomic charges for SiO_2, the aluminosilicates mica and montmorillonite, and tetraalkylammonium ions, including local charge defects by $Si \rightarrow Al^{-}\cdots K^{+}$ and $Al \rightarrow Mg^{-}\cdots Na^{+}$ substitution. Our estimates of atomic charges correlate well with experimental data. Classical force fields based on these charges exhibit up to 1 order of magnitude less error in reproducing crystal geometries (only ∼0.5% deviation in unit-cell parameters), phase diagrams, and interfacial energies.

1. Introduction

In classical atomistic simulations, point charges are defined for each atom. In relatively nonpolar systems, such as hydrocarbons, the atom-based charges only have a minor role; they are of considerable importance in more-polar systems, such as aquatic systems and biomolecules, and are of primary importance in highly polar solids (e.g., aluminosilicates in materials applications). This is the case because (i) they are the only parameters for modeling polarity in classical simulations, and (ii) significant atomic charges (greater than ±1.0) cause the Coulomb energy to supersede terms for bond, angle, or torsion energies in the energy expression typically by ∼2 orders of magnitude. For credible force-field-based simulations, modeling of the electronic distribution on the atomic scale is then as important as modeling correct bond lengths, angles, torsions, vibrational constants, and van der Waals parameters. For example, the structure of interfaces between polar inorganic compounds and charged organic molecules is of the length scale of 1−10 chemical bonds. Atomic charges are typically separated from each other by one chemical bond. On this relative length scale, their value and relative orientation determine the interfacial structure. Particularly, the calculation of adsorption energies is sensitive to the atomic charges.

The importance of adequate atomic charges in simulations has not yet received sufficient attention,[1,2] and computer simulation of polar systems is still a developing area of research. Atomic charges from theoretical approaches often display multiples of scatter and shed doubt on the reliability of corresponding force fields. Improved understanding of the basic factors that determine the polarity of molecules and crystals and ways of obtaining reliable partial charges (with comparisons to accurate experimental measurements of the electron density) would be a significant step forward.

The outline of the paper is as follows. Section 2 is a short review: we examine how charges can be obtained, quote the results of experimental and theoretical methods, and indicate the origin of uncertainties. In section 3, we propose a basic model to analyze the capability of the elements for covalent bonding and for ionic bonding across the periodic table, which leads to an extension of the Born model.[3−6] We specify how the atomization energies and the ionization energies/electron affinities of the elements are helpful in the estimation of semiempirical atomic charges, consistent with experimental determinations of partial charges and dipole moments. In section 4, we discuss trends of the atomization energy and the ionization energies/electron affinities of the elements across the periodic table to illustrate the validity of our arguments. In section 5, as an example, we provide relative charge estimates for SiO_2, mica, montmorillonite,[7] and alkylammonium ions, which are important in materials applications.[8−15] A short validation of our charge estimates in force fields is presented in section 6, and the paper concludes with a summary in section 7.

In addition to atomic charges, the repulsive (and dispersive) van der Waals energies are also needed to generate the nonbond energy between the particles in a classical simulation. In contrast to the electrostatic interaction, the repulsive van der Waals

* Author to whom correspondence should be addressed. E-mail address: hendrik.heinz@wright.edu.

10.1021/jp048142t CCC: $27.50
Published on Web 10/29/2004

TABLE 1: Atomic Charges of (Semi-)Metals in Crystalline Solids from Experimentally Determined Electron Distributions

compound	charge[a]	reference
LiF	0.95 (3)	17
LiI	0.67 (5)	25
NaCl	1.00 (0)	17
KBr	0.8 (1)	18
CaF_2	2.00 (0)	17
MgO	1.6 (2)	16
Al_2O_3	1.32 (5)	22
AlO(OH)	1.47 (27)	19
$AlPO_4$[b]		
Al	1.4 (1)	21
P	1.0 (1)	21
$Cu_6Si_6O_{18}$[c]		
Si	1.17 (15)	24

[a] In units of elementary charge. Values given in parentheses represent the standard deviation of the last digit. [b] The crystal structure is the same as for SiO_2, as surmised with Al and P being the left and right neighbors to Si in the periodic table. The investigation was performed to obtain more information on the charge distribution in the isoelectronic SiO_2, which is pronouncedly noncentrosymmetric. A Si charge of ~1.2 in SiO_2 was inferred (see ref 22). [c] Hydrated by six H_2O molecules.

interaction is only short-range. It can be adjusted by the nonbond radii after the charges have been assigned, and we will not discuss this interaction further in this paper.

2. How Can Atomic Charges Be Determined?

There are two principal ways to determine atomic charges: experimental and theoretical. Experimental methods are usually based on X-ray diffraction (XRD), and theoretical methods can be further divided into ab initio methods and semiempirical methods.

2.1. Experimental Methods. *2.1.1. X-ray Diffraction.* XRD allows the experimental investigation of electron distributions with very high accuracy,[16−25] when compared to theoretical estimates. Although the electron density is a three-dimensional function and often may be anisotropic or noncentrosymmetric around atoms (e.g., in SiO_2),[21] the total electron density can be mapped onto each atom (or an electronic lobe) by integrating the electron density over atomic (spatial) basins, and a corresponding partial charge is calculated (Table 1). Considering the different possibilities available to perform the mapping, the resulting partial charges determined using modern methods are often accurate to within 0.1 e or even 0.05 e,[19−24] depending on the geometry of the electron density in the compound.

2.1.2. Dipole Moments. Dipole moments of small molecules can also be used to calculate atom-based charges with the same precision as that from X-ray data. However, the position of the charges causing the dipole moment and possibly the decomposition of the overall dipole moment into individual dipole moments must be carefully evaluated. In principle, extensive data collections are available.[6]

Experimentally determined charges may be the best basis for parametrizing force fields, using refs 6 and 16−25 or similar data as a starting point. However, alternative methods are needed, because experimental procedures are lengthy and cannot be applied everywhere.

2.2. Theoretical Methods. Theoretical methods can be divided into two groups: (i) the electron density can be calculated in an ab initio way and then partitioned into atomic charges,[26] and (ii) a semiempirical charge equilibration can be employed for a certain family of compounds.[27] Also, empirical approaches or arbitrary combinations have been used, which we illustrate here for aluminosilicates (Table 2). Unfortunately, most methods are of little practical use, because of considerable deviations.

In the following, we quote representative results of the main theoretical approaches and discuss deviations from experimental data. With respect to the performance in force fields, we indicate, for extensively investigated molecules, that only charges similar to the experimental values are suited.

2.2.1. Ab Initio Methods. To calculate the electronic density, e.g., extended Hückel theory,[19,28] Hartree−Fock (HF)-type ab initio methods,[8,29−39] or density functional theory (DFT) methods[40−42] can be used. The partitioning into atomic basins may be performed according to Mulliken analysis (Mulliken charges),[29,30] Bader's gradient method (Bader charges),[31,32] Cioslowski's generalized atomic polar tensor method (GAPT charges),[34,35] other types of partition,[8,37] semiempirical partition,[36] or the method of charges from electrostatic potentials (CHELP charges, respectively CHELPG charges).[33,39] Generally, the particular methods do not yield coherent results, so a wide range of charges for a given system can be predicted. Let us consider two simple examples: the O atom in water (from −0.17[35] to −1.24[31]) and the carbonyl carbon in formaldehyde (from 0.075[35] to 1.36[32]) under standard conditions. A similar spread over multiples can also be found for other inorganic molecules, organic molecules, and organometallic reagents.[2,26] The variation stems from the use of different basis sets with the same partition method (up to 5-fold variation in atomic charge), and the use of the same basis set with different partition methods (up to 5-fold variation in atomic charge). In contrast, we obtain from experiments charges of −0.74(6)[24] (XRD) and −0.66[6,43] (μ) for O in water; a charge of 0.40[6] (μ) is observed for the carbonyl carbon in formaldehyde. For these important molecules, the charges in many force fields (e.g., CHARMM, GROMACS, PCFF, COMPASS, AMBER)[46] have been optimized for decades: elementary charges of −0.48[44] to −0.80[45]

TABLE 2: Atomic Charges Assigned for Simulations of Three Chemically Different Environments: Si in Tetrahedral Oxygen Coordination, Al in Six-Fold Oxygen Coordination, and the Hydroxyl Hydrogen in Aluminate

charge on Si in O_4 coordination[a]	method	reference	charge on Al in O_6 coordination[a]	charge on H in (Al)OH[a]	method	reference
+1.2 (1)	experimental (indirect)	21,22	+1.47 (27)	+0.20 (5)	experimental	19
+1.17 (15)	experimental	24	+1.32 (5)		experimental	22
+4.0	formal charge	47, 48	+3.0		formal charge	10
+3.3	DFT/Mulliken	41	+2.6	+0.12	SCF/partition	8, 37
+2.4	SCF/empirical charge fitting	36, 52	+2.1	+0.44	DFT/Mulliken	42
+1.8	Pauling (1960)	49	+2.1	+0.39	extended Hückel	19
+1.4	semiempirical	9	+1.5−2.0	+0.40	MP2/CHELPG	9, 38
+1.3	charge equilibration	27, 46	+1.7		semiempirical	9
+1.0	Pauling (1980)	50, 51	+1.3	+0.06	SCF/partition/scaling	8, 37
+0.5	SCF/partition/scaling	37	+1.15	+0.25	charge equilibration	27, 46

[a] In units of elementary charge, with the standard deviation of the last digit given in parentheses.

for O in H_2O and 0.40[46] for C in formaldehyde (including the contribution from the two H atoms) are common. The agreement between these values and the experimental data is striking. Different atomic charges have a tendency to falsify coordination geometries, distribution functions, interaction energies, phase diagrams, etc. in the simulation.

The most reliable quantum mechanical tools for relatively good atomic charges are CHELPG[33,39] in combination with second-order Möller−Plesset (MP2)-optimized geometries[38] and certain DFT codes. However, the gap to experimental data can still be large (see Table 2). With the CHELPG method, calculated dipole moments are usually 30% larger than the experimental values[33,39] and we notice an error of a factor of 2 for the hydrogen (see Table 2). DFT results are contingent on the adjustable parameters (pseudopotentials) and may vary substantially (see Table 2). A main problem may be the quantitative incorporation of *d* and *f* electrons and the onset of relativistic effects for elements heavier than the second row in the periodic table.

Overall, the charges from quantum mechanical methods for Si in tetrahedral oxygen coordination (0.5−3.3) and Al in octahedral oxygen coordination (1.3−2.6) are not sufficiently close to experimental data.

2.2.2. Semiempirical Charge Equilibration. An alternative way to obtain partial charges is semiempirical equilibration, such as the widely used method by Rappé and Goddard.[27] It gives usually better results than ab initio techniques. This method is based on electronegativity equalization of the individual atoms of a compound, which was originally formulated for the ionization of gas-phase atoms.[53,54] Ionization potentials and electron affinities of the atoms are taken into account for the electrostatic contributions to the cohesive energy.[27] However, the concept does not incorporate covalent bonding contributions into the cohesive energy, although covalent bonding predominantly contributes to the cohesive energy in organic molecules and is also important in many polar minerals. As we will note below, the capability for covalent bonding varies for each element and strongly influences the atomic charges. To compensate for the neglect of covalent bonding energy in the charge equilibration,[27] corrections for the strength of localized bonding have been made by means of empirical terms and additional reference values, e.g., from available dipole moments.

Therefore, the scope of the method of Rappé and Goddard[27] is limited to a pool of related molecules where a sufficient number of fit parameters have been introduced. For example, charges of good accuracy can be obtained for many organic molecules with common functional groups, which has been very useful. However, the partial charge of ∼0.14 for H in saturated hydrocarbons seems to be overestimated.[44,46] In other systems across the periodic table, deviations may be high and known relationships can be violated. For example, the point charge of Si in tetrahedral oxygen coordination is higher than that of the more electropositive Al in octahedral oxygen coordination[46] (see Table 2). The opposite should be true for both electronegativity and coordination arguments.[51] Such uncertainties and excessive scalings can be relieved by a scientifically more profound concept, satisfying both important aspects of chemical bonding, whereas the idea of a semiempirical charge estimation seems to be best-suited for accurate estimates of partial charges.

In conclusion, the principal question—to what extent can a given structure be considered as a covalent structure and to what extent can it be considered as a dense packing of spherical ions—has not yet been answered sufficiently. Although experimental data provide accurate information, with deviations in elementary charge of approximately ±0.1 (see Table 1), which are suited for force-field parametrizations, theoretical approaches are necessary to obtain charge estimates for a wide variety of compounds easily. The goal of our paper is to provide a basic theoretical understanding of polarity and to allow for semiempirical estimates of atomic charges that come close to the accuracy of available experimental data.

We will not consider further partition of atomic charges, such as replacing atomic point charges by point-charge distributions (dummy atoms), according to orbital geometry, or to introduce interaction parameters between partitioned point charges to model fluctuations.

3. The Extended Born Model[55]

Our considerations on the degree of polarity of a compound are based on the two fundamental types of chemical bonding that constitute the cohesive energy in any solid, liquid, or gaseous compound: localized (covalent) and ionic bonding.

We find purely covalent bonding only in the chemical elements itself; they are composed of electronically identical atoms. The extent of covalent bonding between these atoms is dependent on the number of valence electrons, the shape of the orbitals, atom size, etc. All these effects for each element are contained in the atomization energies ΔH_{at}, which are available for all elements and reflect exactly the energy equivalent to the covalent bonding energy per atom in a homoatomic assembly (Figure 1). We assume that the atomization energies of the individual elements may also be the key to estimate the tendency for covalent bonding between different elements. Covalent bonding tendencies of the elements alone already indicate something about the tendencies of ionic bonding: if covalent bonding is not favorable, ionic bonding would be the only way to form stable compounds; if covalent bonding is strong, ionic bonding would be limited, because the capability for localized bonding would be decreased by charge separation.

To assess the capability for ionic bonding, we refer to the ionization energies ΔU_i and electron affinities ΔU_{ea} of the elements. The analysis of these quantities is known and formed the basis of Pauling's electronegativity scale.[53] The ionization energy (first, second, ...) is the energy required to remove electrons and the negative electron affinity (first, second, ...) is the energy obtained by the uptake of electrons. The energetic balance $\Delta U_i - \Delta U_{ea}$ is thus a measure of the energy required for a given degree of charge separation in a compound. Which part of the compound is thereby positively polarized and which part is negatively polarized can be judged from chemical experience, electronegativity rules, or, most accurately, from the energetic minimum of the (two) possible balances $\Delta U_i - \Delta U_{ea}$. If the quantity is low for significant charges, a high polarity is expected, especially when ΔH_{at} is low. If this quantity is high for modest charges, a low polarity is expected, especially when ΔH_{at} is high.

The two discussed contributions are our basis for a semiempirical understanding of polarity, and their role becomes clearer in an extended Born model. This is now derived from the Born model of ionic solids, which is not valid for compounds with covalent bonding contributions.

3.1. The Born Model, Its Shortcomings, and the Necessity for Extension. A thermochemical cycle was proposed by Born[3] and further developed by Haber in 1919.[4,5] Starting with the cleavage of an ionic compound into the elements, the elements are atomized, the atomized elements are ionized to formal charges, and the charged gas-phase atoms are condensed into a purely ionic lattice, arriving at the starting point of the cycle.

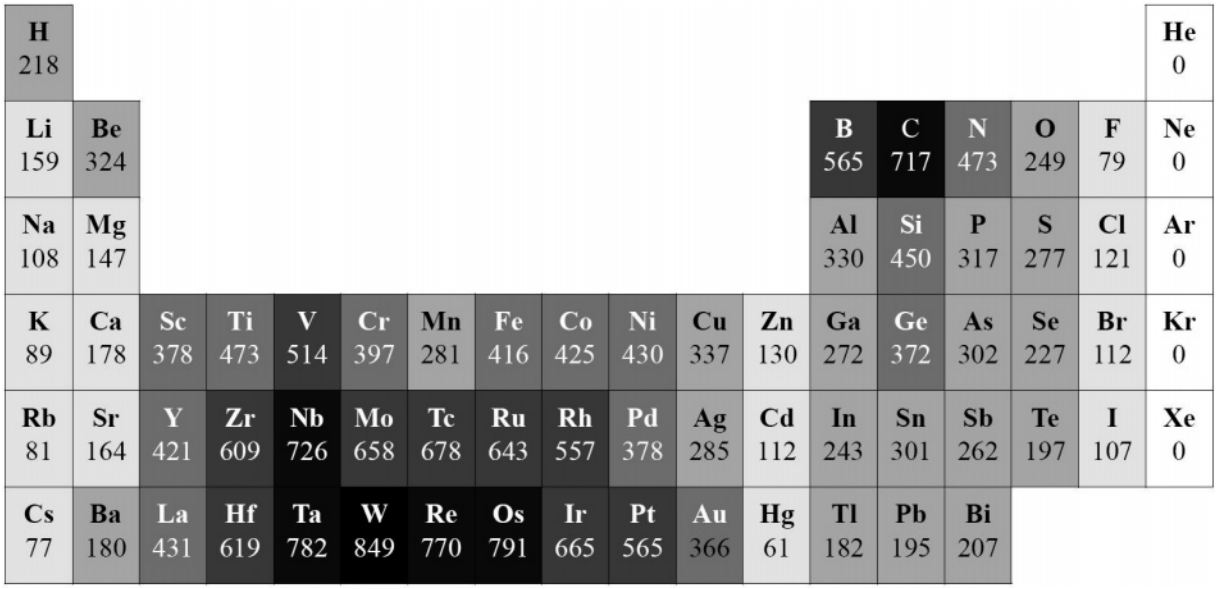

Figure 1. Atomization enthalpies of the elements, in units of kJ/mol atoms, according to ref 6. The values correlate with the tendency for covalent bonding, as illustrated by the darker background. The highest values in the main group are found for boron, carbon, nitrogen, and silicon. The maximum is reached for heavy transition metals (such as tungsten).

For binary salts, lattice enthalpies[56] can be calculated according to the contributions of electrostatic attraction and van der Waals repulsion at small interatomic distances:[3−5,53]

$$\Delta H_{\mathrm{el}} = \frac{N_{\mathrm{A}} \alpha q_i q_j e^2}{4\pi\epsilon_0 r_0}\left(1 - \frac{1}{n}\right) \qquad (1)$$

where N_{A} is the Avogadro constant; α is the Madelung factor for the respective crystal lattice; q_i and q_j are the partial charges of the cation and anion, respectively; e is the elementary charge; r_0 is the distance between the cation and the anion; and n is an empirical quantity between 5 and 12 that approximates the distance dependence r^{-n} of the repulsive energy.[3,53] The lattice enthalpy can also be independently calculated when the first three contributions are known (cleavage into elements, atomization, ionization to full formal charges) as the remaining contribution in the closed thermochemical cycle. Born found that the cohesive energy according to the calculated lattice energy in eq 1 and that determined according to thermochemistry are in good agreement for any of the binary salts.[3,4] This finding has been regarded as evidence for full ionization in the binary salts.[5]

However, this conclusion is not true: Full formal charges are assumed as a matter of course in both independent calculations. Formal charges are inserted in eq 1, as well as the experimentally measured interionic distance r_0; therefore, we obtain a cohesive energy for a hypothetically fully ionic solid. Ionization to full formal charges is also assumed in the thermochemical cycle; therefore, the resulting cohesive energy is also the value for a hypothetically fully ionic solid. Hence, good agreement between the two independently calculated lattice energies is expected, as a "thermochemical application of the lattice theory" (title of ref 3). The real polarity of the solid is never considered and may actually range from fully ionic to strongly covalent. Minor deviations between the two calculated lattice energies values are observed, because the enthalpy of formation in the thermochemical cycle is dependent on the real polarity of the compound, and eq 1 is, to some degree, approximate, because of the row-dependent exponent n for the repulsive energy, as well as the interionic distance r_0 inserted from experiment. When the real structure is not fully ionic, r_0 also may be slightly different.

Therefore, the Born model does not provide information about the polarity of a compound. The a priori assumption of formal charges is justified for several alkali halides, although even there we find noticeable deviations (see Table 1 and section 4.1). In most instances, compounds are significantly covalent (see Table 1). The "lattice energies" in the original Born model, according to eq 1, represent only hypothetical values for the case of completely ionic bonding; nevertheless, they are presently still in use (see the section on lattice enthalpies in ref 6), as well as full formal charges in force fields for solids with highly covalent character.[10,47,48,65] An extension of the Born model, which contains all the known basic constants to describe the polarity of a compound, is necessary to describe compounds in a physically correct manner.

3.2. The Extended Born Model. The extension of the Born model, which reflects the various degrees of polarity, is presented in Figure 2. The cycle starts with cleavage of the compounds into the chemical elements in their natural modification, the elements are atomized, the atomic elements are ionized to atomic charges that may take any value between zero and the formal charges, then the ionized atoms condensate to form the compound with the repective electrostatic bonding contribution and the respective covalent bonding contribution to the cohesive energy, arriving at the starting point of the cycle. The new component is that we allow for a partial ionization, corresponding to the polarity of the real compound, and that we divide the cohesive energy into an electrostatic component that is due to the atomic charges and a covalent component that is due to the formation of localized bonds at the same time. From purely ionic bonding to purely covalent bonding, all transitions are covered by this framework.

Before proceeding with the discussion of the individual energy contributions, we state more precisely our understanding of atomic charges. The customary anisotropy of the electron density (cf. section 2.1)[20] makes an absolutely stringent definition impossible when looking very closely at any compound. Nevertheless, we consider partial charges on each atom as the difference between spherical integrals over the valence electron

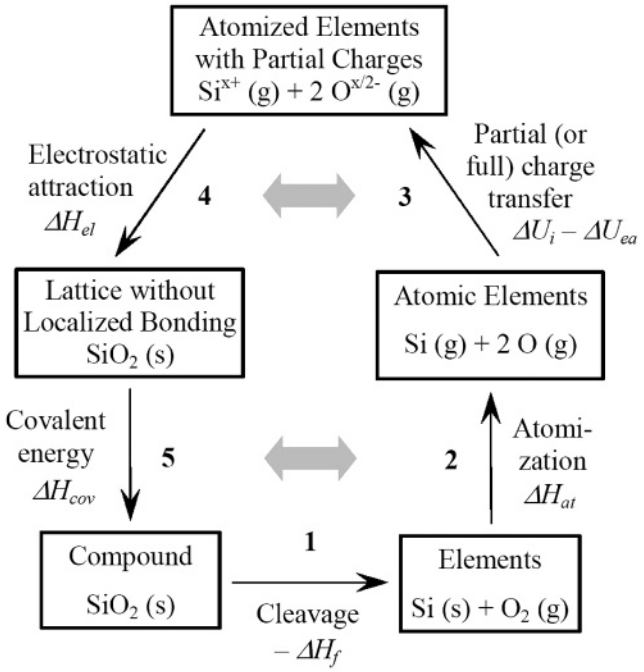

Figure 2. Extended Born model for the example of silicon dioxide (SiO_2). Single-headed arrows describe reversibly taken steps, as indicated in the text. Partial ionization energies and electron affinities are involved in step 3. The lattice energy is divided into an electrostatic/repulsive component in step 4 plus a covalent component in step 5. The respective stoichiometric coefficients must be remembered. The shaded, double-headed arrows indicate the complementary electrostatic (top) and covalent (bottom) contributions to the cycle.

density of the neutral atom and the valence electron density of the same atom in a compound. The sum of these integrals over all atoms in the compound is normalized to the total number of valence electrons in this compound. Collectively, the spherical integrals thus account for all valence electrons and should comply with the experimental electron-density map in the best possible way. We have shown (section 2) that, in modern experiments,[20−24] the accuracy of such assignments usually does not fall below 0.1 e.

Now, we consider the energy contributions in the extended Born model in detail (see Figure 2). The first step is the overall decomposition of a compound or a structural unit into the elements. The associated enthalpy is the negative enthalpy of formation, $-\Delta H_f$. For stable inorganic and organic compounds, the average enthalpy of formation per atom is approximately a constant that is dependent somewhat on the overall polarity. $-\Delta H_f$ is 0.0 ± 0.1 MJ/mol atoms for organic compounds and 0.3 ± 0.1 MJ/mol atoms for the utmost ionic alkali and alkali-earth fluorides, chlorides, and oxides.[6] The second step in the extended Born cycle is the conversion of the elements into isolated gaseous atoms by sublimation or dissociation; the associated enthalpy is ΔH_{at}. The value per atom is in the range of 0.0−0.85 MJ/mol atoms (see Figure 1). In step 3, the atoms are ionized toward the realistic partial charges, which we want to estimate later. The ionization requires partial ionization energies for the cationic component and releases partial electron affinities for the anionic component. These quantities can be estimated on the basis of Tables 3 and 4,[6] with a physical approximation for fractional charges. We designate the energetic balance for this step as $\Delta U_i - \Delta U_{ea}$, and this contribution does usually not exceed 0.7 MJ/mol atoms for a small electroneutral structural unit (see also section 4.2). In steps 4 and 5, the gaseous ions condense to form the solid; we separate the cohesive energy into two parts. In step 4, only the electrostatic energy ΔH_{el} resulting from the partial charges is released. It can be calculated according to eq 1. In step 5, the energy contribution ΔH_{cov} of localized bonding is added.

TABLE 3: Atomization Enthalpy (ΔH_{at}) and the First Three Ionization Energies (all in MJ/mol atoms) for Selected Elements in the Periodic Table[a]

	element	ΔH_{at}	ΔU_i^I	ΔU_i^{II}	ΔU_i^{III}
row 2	Li	0.16	0.52	7.30	11.81
	Be	0.32	0.90	1.76	14.85
	B	0.57	0.80	2.43	3.66
	C	0.72	1.09	2.35	4.62
row 3	Na	0.11	0.50	4.56	6.91
	Mg	0.15	0.74	1.45	7.73
	Al	0.33	0.58	1.82	2.74
	Si	0.45	0.79	1.58	3.23
	P	0.32	1.01	1.90	2.91
row 4	K	0.09	0.42	3.05	4.41
	Ca	0.18	0.59	1.15	4.91
	Zn	0.13	0.91	1.73	3.83
	Ga	0.27	0.58	1.98	2.96
	Ge	0.37	0.76	1.54	3.30
	As	0.30	0.94	1.80	2.74

[a] From ref 6.

TABLE 4: Atomization Enthalpies (ΔH_{at}) and Electron Affinities (ΔU_{ea}) of Some Nonmetals

	element	ΔH_{at} (MJ/mol atoms)[a]	ΔU_{ea} (MJ/mol atoms)[b]	
row 2	N	0.47	0.01	N^{1-}
			−0.67	N^{2-}
	O	0.25	0.14	O^{1-}
			−0.74	O^{2-}
	F	0.08	0.32	
row 3	Cl	0.12	0.35	
row 4	Br	0.11	0.33	
row 5	I	0.11	0.30	

[a] From ref 6. [b] From ref 53.

Every step in the cycle is taken reversibly, and the cycle leads back to the starting material. Thus, the sum of changes of the thermodynamic state functions over all steps amounts to zero (e.g., internal energy U, enthalpy H, entropy S, and Gibbs' energy G):

$$\sum_i \Delta U_i = \sum_i \Delta H_i = \sum_i \Delta S_i = \sum_i \Delta G_i = 0 \qquad (2)$$

The enthalpy of formation for a compound is contained in steps 2−5,[56]

$$\Delta H_f = \Delta H_{at} + (\Delta U_i - \Delta U_{ea}) + \Delta H_{el} + \Delta H_{cov} \qquad (3)$$

and can be divided into the "ascending" and "descending" pathways presented in Figure 2. The processes of atomization and ionization require energy. The cohesive process delivers electrostatic and covalent lattice energy to the environment.

ΔH_{at} signifies a purely covalent energy, because no charge separation exists between atoms of the same element, and the atomization enthalpy contributes fully in every cycle. In contrast, $(\Delta U_i - \Delta U_{ea})$ is caused by charge transfer between a group of isolated atoms; this energy is determined by the atomic charges in the compound. Upon condensation, the electrostatic energy of ionization is returned as electrostatic lattice energy ΔH_{el} for

TABLE 5: Indicators for Partial Charges in Polar Solids, Given in Order of Decreasing Relevance

	ionic bonding	covalent bonding
atomization enthalpy, ΔH_{at}	small (<0.2 MJ/mol atoms)	large
ionization energies and electron affinity, $\Delta U_i - \Delta U_{ea}$	small	large
polarizability	small	large
coordination numbers in equal electronic configurations	large	small
preferred solvents	polar	nonpolar
melting points of compounds with low ΔH_{at} (only ΔH_{el} prevents melting)	high	low
dipole moments (if no vectorial cancellation)	large	small

the entire crystal; it may be estimated according to eq 1. Finally, the covalent energy of atomization is recuperated as covalent lattice energy ΔH_{cov}; however, the magnitude is dependent on the electronic structure (orbitals, coordination in the solid) and the number of valence electrons available after ionization. Altogether, there are two ionic contributions, namely, ionization of single atoms in step 3 versus the release of electrostatic energy of the entire lattice in step 4, as well as two covalent contributions, namely, cleavage of homoatomic bonds in step 2 versus the formation of (partial) heteroatomic bonds in step 5.

The extent of covalent and electrostatic contributions to bonding is determined by the relative values of the atomization energy (see Figure 1) and the ionization energy/electron affinity ($\Delta U_i - \Delta U_{ea}$; see Tables 3 and 4):

(1) If the atomization energies of the constitutent atoms are small, no significant covalent bonding is possible a priori and the cohesive energy of a stable solid must be primarily ionic, e.g., in alkali halides. In case the ionization energies and the negative electron affinities are too high, little driving force for compound formation remains, e.g., for noble gas compounds.

(2) If the atomization energies of the constituent atoms are high, this covalent potential helps in the condensation process (step 5 in Figure 2). It will be complemented by a degree of ionic bonding, depending on the quantity $\Delta U_i - \Delta U_{ea}$. However, strong electrostatic bonding is limited, because it diminishes the available valence electron density for beneficial localized bonding. This is the case, e.g., for carbon compounds or certain transition-metal compounds (see Figure 1).

To calculate atomic charges directly from the extended Born cycle, we need to know the energies for all steps (1−5), as a function of the atomic charges. Satisfaction of eq 3 would be achieved for the appropriate values of the partial charges. This approach, if performed with high precision, is probably the most accurate and may involve ab initio calculations to evaluate the energies of steps 3−5. For a faster and simple semiempirical equilibration, ΔH_{cov} can be crudely estimated as the part of the atomization energy ΔH_{at} that remains after ionization (step 3), according to the reduced number of valence electrons available for localized bonding, ΔH_{el} is given by eq 1, and the other contributions are known or derived from tabulated values. However, a more suitable approach, with respect to accuracy, is to use available reference compounds (see Table 1), taking advantage of accurate experimental charge determinations. The quantities in the extended Born cycle, especially ΔH_{at} and $\Delta U_i - \Delta U_{ea}$, then form the basis to derive accurate atomic charges, relative to these reference compounds.

Other properties such as polarizabilities, coordination numbers, melting points, solubilities, or dipole moments are additional indicators of polarity and partial charges. Moreover, any other relationship between physical properties or chemical reactivity and polarity may be consulted. The determining factors of atomic charges within a compound or a structural unit, in relation to reference compounds, are listed in Table 5.

4. Periodic Trends in Atomic Charge Assignments

4.1. Alkali Halides Revisited: Covalent Bonding Contributions. It is worthwile to re-examine the alkali halides, which were the subject of Born's study.[3,4] While relatively few experimental investigations on the electron density in the solids have been performed (see Table 1), the charges of binary alkali halide molecules in the gas phase are well-known from dipole moments.[27] These values are likely to correlate with the corresponding point charges in solids, because the crystal structures are often almost identical. Evaluating these data in Table 1 and in ref 27, we conclude that LiF, NaF, KF, NaCl, KCl, and perhaps RbCl and RbF have a cation charge greater than +0.95, whereas the cation charge of the remaining alkali halides is smaller, with a minimum near +0.67 for LiI. This trend correlates with a decrease of melting points (Table 6). With a larger cation or anion, e.g., Rb, Cs, Br, or I, the increased polarizability introduces considerable covalent bonding contributions. In conclusion, only a minority of the solid alkali halides exhibits full formal charges.

When the partial charges are given, the covalent cohesive energy ΔH_{cov} (see Figure 1) can be estimated using eqs 1 and 3. We illustrate this for the example of LiI with atomic charges of ±0.67 (see Table 1). Using a Madelung constant of $\alpha = 1.748$ for a 6:6 lattice, $r_0 = 301$ pm,[6] and $n = 9$, we obtain an electrostatic cohesive energy of $\Delta H_{el} = -0.32$ MJ/mol from eq 1. The enthalpy of formation is $\Delta H_f = -0.270$ MJ/mol,[6] and the total atomization energy is $\Delta H_{at} = 0.27$ MJ/mol (see Tables 3 and 4). The energy for ionization $\Delta U_i - \Delta U_{ea}$ must be approximated for the given partial charges. We assume here a linear scaling of the first ionization potential of Li and the electron affinity of I, with the corresponding charge of 0.67 (Table 4) for simplicity, leading to $\Delta U_i - \Delta U_{ea} = 0.67(0.52-0.30)$ MJ/mol = 0.15 MJ/mol, although the shape of this function often needs careful analysis (see section 4.2). Using eq 3, it follows that $\Delta H_{cov} = -0.37$ MJ/mol. Therefore, the cohesive energy for LiI, $\Delta H_{el} + \Delta H_{cov} = -0.69$ MJ/mol, is ∼50% covalent.

TABLE 6: Melting Points (K) of Some Metal Halides[a]

	group Ia				group IIa				group IIb	group IIIa
	Li	Na	K	Rb	Be	Mg	Ca	Sr	Zn	Al
fluoride	1121	1269	1131	1106	825	1536	1691	1750	1145	1563
chloride	883	1073	1044	988	688	987	1048	1147	548	465

[a] From ref 6. Substantially lower melting points, relative to KF, NaCl, or CaF_2 within a related group indicate lower partial charges, compared to the formal charges (see text).

4.2. General Periodic Trends. Now, we discuss in more detail the main indicators of polarity, to illustrate their influence on atomic charges (see Table 5). Some results will also be useful in section 5.

4.2.1. Atomization Enthalpies. The most apparent criterion to evaluate the extent of covalent bonding in solids are the atomization enthalpies[56] of the elements (see Figure 1). The elements with the largest atomization enthalpies have the smallest partial charges and the strongest covalent character; they are relatively inert chemically and form a wide variety of stable compounds. Examples are carbon, boron, nitrogen, and silicon from the main group, as well as several d-electron metals, which may also form multiple bonds with carbon (Ta, W, Os).[57] The chemistry of these elements is dominated by the high number of available valence electrons. On the other hand, alkali metals and the halogens with the smallest atomization enthalpies have the largest charges and prefer ionic lattices; they are very reactive and yield a much smaller number of compounds. These tendencies are linked to the low number of valence electrons. For example, with only 1 valence electron available to create covalent bonds to 12 neighbors in solid alkali metals, the bonding forces are weak and, consequently, the melting points are low. In alkali halides with coordination numbers of 6 or 8, only the possibility of ionization and subsequent strong Coulomb attraction stabilizes the compounds.

With increasing atom size and polarizability, as well as populated *d*-orbitals for interaction, the covalent character may increase to become comparable to the electrostatic one, as shown above for LiI, although atomization energies, ionization potentials, and electron affinities are almost the same (even with a small tendency of diminution; see Tables 3 and 4). Another example for the correlation of atomization energy with covalent bonding tendency is the trend from the alkali metals toward alkali-earth metals and from halogens toward chalcogens. The atomization energy increases in both cases (see Figure 1, Tables 3 and 4) and the concomitant increase in covalent character is illustrated by the emergence of relatively stable organometallic compounds (Grignard reagents) and polymeric structures ($BeCl_2$), as well as from the lower electron affinity of oxygen (Table 4) with a maximum at a negative charge of -0.6 to -0.7.[53] Full formal charges are disfavored and the tendency of covalent bonding increases when there are more bonding electrons available. Analysis of the electron density of MgO shows partial charges distinctly lower than ± 2 (see Table 1),[17] whereas the isoelectronic NaF is fully ionic.[27]

4.2.2. Ionization Enthalpies and Electron Affinities. Changes in ionization enthalpies and electron affinities within a row or a column of the periodic table affect the charges. If the ionization enthalpy increases significantly, the partial charges decrease. This can be illustrated by the sum of the two first ionization energies of Ca, Mg, and Be: 1.74, 2.19, and 2.66 MJ/mol, respectively. CaF_2 has full charges of $+2$ and -1 (see Table 1), but its high melting point decreases somewhat toward that of MgF_2 and sharply toward that of BeF_2 (see Table 6). The same trend appears for the respective chlorides. The conclusion is that MgF_2 has a slightly decreased charge of 1.8, and we may assume a low charge of ~ 1.0 for BeF_2, which has the same structure as quartz (SiO_2).[25] Support comes also from the change in coordination numbers from 8:4 via 6:3 toward 4:2 and the relative increase of $(\Delta H_{at} + \Delta U_i^{I} + \Delta U_i^{II})$ from CaF_2 to BeF_2 (1.93, 2.35, and 2.98 MJ/mol, respectively). The partial charges in the corresponding alkali-earth chlorides are presumably approximately $+1.3$, because of their generally lower melting points and concomitantly different crystal structure (see Table 6). The Be point charge is probably as low as $+0.8$ in $BeCl_2$, which forms a covalent polymeric $(BeCl_2)_x$ chain. The small partial charges on beryllium are also supported by the amphoteric behavior of the hydroxide $Be(OH)_2$, in relation to the increasing basicity of the hydroxides of magnesium, calcium, strontium, and barium.[25]

Similarly, a strongly negative electron affinity (e.g., -0.74 MJ/mol for O^{2-}; see Table 4) disfavors a high negative charge of -2.0, even if the counterion is an alkali metal. The main difference between oxides and halides is that oxygen has a maximum of its electron affinity of ~ 0.2 MJ/mol for a charge between -0.6 and -0.7, whereas the electron affinity for halogens may be highest for a full negative charge of -1 (see Table 4). If oxygen accommodates a charge of -2, an energy of 0.6 MJ/mol is required, whereas two halide ions with charges of -1 release an energy of 0.65 MJ/mol. Therefore, oxygen always preserves some covalent bonding[53] while there is a strong tendency toward modest negative charges. The trend to covalent bonding is reflected in the higher atomization enthalpy.

4.2.3. Polarizability. The polarizability of the elements correlates with the sum of ionization energy and electron affinity. Especially for nonmetals, we find an increase with higher row number in the periodic table, associated with a decrease in the first ionization energy. A particular gap from the second row to the third row[6] makes any compound with Cl or Br more covalent than compounds with F. From dipole moments,[6] e.g., we obtain partial charges of carbon in CH_2F_2, $(H_2CO)_3$ (trioxane), and CH_2Cl_2 of $+0.52$, $+0.39$, and $+0.34$, respectively.

As a conclusion of the previous arguments, elementary charges larger than $+2$ or -2 are unusual (except for molecules of extreme polarity, such as UF_6). Compounds from elements, which donate or accept more than two valence electrons, gain their cohesive energies mainly from covalent bonding contributions (see the larger atomization energies in Figure 1). However, the electrostatic component is important and can be described by atomic charges.

5. Atomic Charges in Mica, Montmorillonite, and Tetraalkylammonium Ions

We consider SiO_2 and two representative aluminosilicates with amphiphilic surfactants as examples, which are important for advanced nanocomposite materials.[8−15] For charge estimates with our method, we primarily need a good understanding of the structural units in the minerals. The formulas are $K[Al_{0.25}Si_{0.75}O_2]_4[AlO(OH)]_4[O_2Si_{0.75}Al_{0.25}]_4K$ for muscovite mica and $Na_{0.4}[SiO_2]_4[Al_{0.8}Mg_{0.2}O(OH)]_4[O_2Si]_4Na_{0.4}$ for a typical Na-montmorillonite.[7] The formulas are written in the order of the joint layers constituting one lamella.[15a,25] First, there is a tetrahedral layer, which has the composition of silicon dioxide (SiO_2). In case of mica, one out of four Si atoms is replaced by an Al atom ($Si \rightarrow Al^{-}\cdots K^{+}$). Second, O atoms that point from the even surface of this tetrahedral layer to the lamella center are connected to Al atoms of an internal octahedral aluminum oxide−hydroxide layer. In the case of montmorillonite, some of the Al atoms are replaced here by Mg atoms ($Al \rightarrow Mg^{-}\cdots Na^{+}$). Third, this layer, with an octahedral coordination of the Al or Mg atoms, is, in turn, connected to another tetrahedral layer, which is identical in composition to the first. The rigid unit of the three discussed layers forms a sandwich-like lamella. Between the lamellae sit the alkali counterions. They compensate the valence electron deficiency in the lamellae caused by the $Si \rightarrow Al$ or $Al \rightarrow Mg$ metal replacements.

We consider first SiO_4 tetrahedra in the SiO_2-like structure (unsubstituted tetrahedral layer) and $Al(O, OH)_6$ octahedra in

TABLE 7: Value of the Quantity $\Delta H_{at} + \Delta U_i - \Delta U_{ea}$ for SiO_2 and the Group of Alkali-Earth Halides MgX_2 and CaX_2 (for X = F, Cl) for Assumed Charges of 0, +1, and +2

	$\Delta H_{at} + \Delta U_i - \Delta U_{ea}$ (MJ/mol)	
charge	SiO_2	MgX_2, CaX_2
0	0.95	0.3−0.4
+1	1.46	0.6−0.8
+2	3.04	1.5−1.9

the AlO(OH)-like structure (unsubstituted octahedral layer). We then discuss the local charge imbalances by $Si \rightarrow Al^- \cdots K^+$ and $Al \rightarrow Mg^- \cdots Na^+$ substitution. A Si charge of ~1.2[21,22,24] and charges of ~1.4 for Al and 0.2 for hydroxyl H[19,22] have been determined independently by experiment (see Table 2), whereas no treatment for charge defects is available.

5.1. Charges in the Unsubstituted Tetrahedral and Octahedral Layers. We develop five independent arguments to estimate the Si charge in SiO_2 with 4/2 coordination and three more arguments for the Al charge in the aluminate, based on our theoretical concept.

5.1.1. Argument (1). The Mg charge in MgF_2 amounts to +1.8, based on experimental data (section 4.2). Atomization energies for both Mg and F in MgF_2 are substantially lower than that for Si and O in SiO_2 (see Figure 1); as an average over the three atoms, we obtain an atomization energy of 0.10 MJ/mol atoms for MgF_2, compared to 0.32 MJ/mol atoms for SiO_2. We then expect a Si charge lower than +1.8 in SiO_2, also supported by the decrease of coordination numbers from 6/3 to 4/2.

For a more careful estimate, we evaluate the sum $\Delta H_{at} + \Delta U_i - \Delta U_{ea}$ from steps 2 and 3 of the extended Born model (see Figure 2) for stepwise Si charges of ±0, +1, and +2 (Table 7). An assumed Si charge of ±0 yields 0.95 MJ/mol for SiO_2 and 0.3−0.4 MJ/mol for heavier alkali-earth fluorides and chlorides. The difference of 0.6 MJ/mol reflects the higher potential of SiO_2 for covalent bonding (more valence electrons). In both compounds, the ionization potentials/electron affinities of the constituents are unequal, so we expect a certain ionization for optimum cohesion. An assumed Si charge of +1 yields 1.46 MJ/mol for SiO_2 and 0.6−0.8 MJ/mol for heavier alkali-earth fluorides and chlorides (see Table 7).[58] The difference is in the same range as the difference in covalent bonding but has increased to 0.75 MJ/mol. Knowing that the charges in $CaCl_2$ and $MgCl_2$ do not exceed +1.3 (section 4.2), we conclude that the Si charge hardly exceeds +1.0. An assumed Si charge of +2 yields 3.04 MJ/mol for SiO_2 and 1.4−1.9 MJ/mol for heavier alkali-earth fluorides and chlorides (see Table 7).[58] The gap of 1.3 MJ/mol, relative to MgF_2, is much larger than the remaining ~0.5 MJ/mol of covalent energy of SiO_2 at an assumed charge of +2. Thus, the ionization of SiO_2 will be sharply less than +2 (even in MgF_2 ionization, it is limited to +1.8). As an overall conclusion, we estimate a Si charge of +1.1 (±0.3) for Si in SiO_2.

5.1.2. Argument (2). Since carbon and silicon are neighbors in the periodic table, a comparison is helpful. A C−O−C single bond with a bond length of 142 pm in dimethyl ether effects a charge of +0.17 on carbon and the O−C−O bonds in cyclic acetals +0.39, as obtained from experimental dipole moments.[6] If carbon would be tetrahedrally coordinated by oxygen, its approximate charge might be +0.80. For silicon with lower atomization energy and lower first ionization energy (see Table 3), compared to carbon (1.24 MJ/mol versus 1.81 MJ/mol), the charge should be larger, despite an increased polarizability, at ~1.1 (±0.2).

5.1.3. Argument (3). For a SiO molecule with a bond length of 151 pm, a charge of +0.43 is found from dipole moments.[7] This bond has somewhat greater double-bond character than the bonds in solid SiO_2 or aluminosilicates with a bond length of 161 pm. If we crudely assume additivity, we obtain +0.86 as a maximum charge for a hypothetical SiO_2 gas. This charge would increase with the higher coordination number of four in solid SiO_2. Such an increase was estimated to be ~40%.[51] It follows a Si charge of +1.2 (±0.3) in SiO_2.

5.1.4. Argument (4). BeF_2 and SiO_2 have the same stoichiometry and crystal structure.[25] The Be−F and Si−O bond distances are both equal to 160 pm. The sum of atomization energies, first ionization energy, and negative electron affinity ($\Delta H_{at} + \Delta U_i - \Delta U_{ea}$) for an assumed metal charge of +1 is 1.46 MJ/mol for SiO_2 and 1.06 MJ/mol for BeF_2.[25] The difference is equal to the remaining covalent energy for the given charge: $(0.75\Delta H_{at}(Si + 2O) - 0.5\Delta H_{at}(Be + 2F) = 0.46$ MJ/mol). Therefore, we assume the same partial charge of +1.0 (±0.3) for Si in SiO_2 as +1.0 for Be in BeF_2 (cf. section 4.2).

5.1.5. Argument (5). When comparing zinc halides to alkali-earth halides, the melting points indicate significant covalent character (see Table 6), especially relative to CaF_2 with a partial charge of +2.0 for Ca. The partial charge may be +1.4 in ZnF_2, which coordinates octahedrally and is hygroscopic, but is only +0.7 in $ZnCl_2$, which coordinates tetrahedrally and is soluble in organic solvents. Because the sum of atomization and ionization energies for zinc is similar to that for silicon and aluminum (see Table 3), we anticipate similar atomic charges. Taking into account the slightly higher atomization energy of oxygen, compared to that of fluorine and a lesser polarizability than chlorine, a Si charge near +1.1 (±0.3) for Si in SiO_2 is likely.

The outcomes of arguments (1)−(5) are very similar, and, therefore, the most likely Si charge in SiO_2 is +1.1 (±0.2). When compared to experimental assignments (see Table 2), this value is within the specified error. Because the electronic environment in the tetrahedral layer of phyllosilicates is very similar to that of SiO_2, we assume this charge for Si in the tetrahedral layer of aluminosilicates, together with an average oxygen charge of −0.55 (when O is not bonded to Al at the same time).

5.1.6. Argument (6). The metal−nonmetal bond lengths for MgF_2, AlF_3, and AlO(OH) are very similar,[53] and the metal coordinates octahedrally in all three compounds.[25] AlF_3 melts at a temperature similar to that of MgF_2 (see Table 6), and MgF_2 has a charge of +1.8 (section 4.2). Evaluating the quantity $\Delta H_{at} + \Delta U_i - \Delta U_{ea}$ for an assumed metal charge of +2, we find ~2.3 MJ/mol for AlF_3 and 1.86 MJ/mol for MgF_2. The "remaining" covalent energy amounts to ~0.2 MJ/mol for AlF_3 and 0.0 MJ/mol for MgF_2, which does not fully compensate the difference in $\Delta H_{at} + \Delta U_i - \Delta U_{ea}$. We then expect a slightly lower charge of +1.6 in AlF_3.[59] $AlCl_3$ melts significantly lower than AlF_3 (see Table 6), because of a change of the coordination number from 6 to 4 during melting and predominantly covalent character. It is soluble in benzene and chloroform,[25] and the Al charge is probably only +0.8. Because the oxygen and hydroxyl in AlO(OH) are somewhat more covalent than fluorine, less polarizable than chlorine, and do not display properties similar to $AlCl_3$, we estimate the Al charge in octahedral O coordination as +1.4 (±0.3).

5.1.7. Argument (7). Having established the Si charge of 1.1 in SiO_2, we can estimate the Al charge in AlO(OH) by augmenting the coordination number and substituting the element. The additional hydroxyl H in the aluminate compen-

TABLE 8: Partial Charges for Mica, Montmorillonite, and Tetraalkylammonium Ions[a]

atom type	charge	estimated deviation
Tetrahedral Layer		
Si	+1.1	±0.1
Al-defect	+0.8	±0.2
O on the surface[b]	−0.55	±0.1
when also bonded to Al-defect[b]	−0.78333	
Octahedral Layer		
Al	+1.45	±0.1
Mg-defect	+1.1	±0.2
O connected to tetrahedral layer[b]	−0.75833	±0.1
when also bonded to Mg-defect[b]	−0.86666	
O connected to H[b]	−0.68333	±0.1
when also bonded to Mg-defect[b]	−0.79166	
H	+0.20	±0.1
Interlayer		
alkali cations (Li^+, Na^+, K^+)	+1.0	−0.1
Tetraalkylammonium Ions		
N	−0.10	±0.1
C when connected to ammonium N	+0.275[c]	±0.025

[a] In units of elementary charge. Mica usually has no Mg-defects, and montmorillonite usually has no Al-defects. [b] The excessive decimals for oxygen are given to maintain charge neutrality. [c] This charge may be partly spread over adjacent H atoms.

sates for the reduced number of valence electrons in Al and enables a regular 6/3 coordination for Al/O.[25,59] The transition from tetrahedral to octahedral coordination increases the charge by ∼25%,[51] yielding a value somewhat less than +1.4. The sum of atomization and the first ionization energy of Al is lower than that for Si (0.91 MJ/mol versus 1.24 MJ/mol), which increases the Al charge to ca. +1.5. The hydroxyl H, which has a slightly positive charge, hardly reduces the Al charge, because ·OH itself is a strongly electronegative unit. Thus, we estimate the resulting Al charge to be +1.5 (±0.3).

5.1.8. Argument (8). The charge on the H atom can be derived from dipole moments of gas-phase water and the hydroxyl radical.[6] We obtain values of +0.33 and +0.36, respectively,[43] in agreement with a value of ($\Delta H_{at} + \Delta U_i^I$) between C and Si (a C charge of +0.17 and a Si charge of +0.43 has been observed for similar coordinations; see arguments (2) and (3)). However, the hydroxyl O atom in the minerals is bonded further to two Al atoms and not to a second H atom such as that observed in water.[45] The two electropositive Al atoms transfer significantly more electron density to the oxygen than a single H atom in water, so that the charge on the H atom in the aluminate is reduced, in agreement with experimental measurements (see Table 2), to a value of +0.20.

Overall, we note a good agreement of arguments (6)−(8) with data from experiment (see Table 2), and we assign atomic charges of +1.45 to Al and +0.20 to H. The remaining charges of O in the octahedral layer are now assigned commensurate to their connectivity and the coordination numbers of their neighbors. Two-thirds of the O atoms in the octahedral layer are bonded to two Al atoms and one Si atom, and one-third is bonded to two Al atoms and one H atom. The first set of O has $^2/_6$ of the Al charge plus $^1/_4$ of the Si charge (i.e., −0.75833), and the OH oxygens have $^2/_6$ of the Al charge plus $^1/_1$ of the H charge (i.e., −0.68333; see Table 8). The excessive number of decimals serves the purpose of overall charge neutrality. Because the difference between the two sets of O atoms is not large, a weighted average of −0.73333 for all O atoms in the octahedral layer might also be used.

5.2. Local Charge Defects. In the tetrahedral layer of mica, approximately every fourth Si atom is replaced by an Al atom. In the octahedral layer of montmorillonite, approximately every fifth Al atom is replaced by a Mg atom. It is highly unlikely that these defects are adjacent in the crystal lattice, such as Al−O−Al contacts in the tetrahedral layer and Mg−O−Mg contacts in the octahedral layer, because they would increase the internal energy of the lattice. The absence of Al−O−Al contacts in the tetrahedral layer of mica (Loewenstein's rule) was proven by ^{29}Si NMR,[60] and we also assume the absence (or rarity) of Mg−O−Mg contacts in the octahedral layer. The separation of the AlO_2^- and $MgO(OH)^-$ units by at least one (nondefective) Si or Al atom allows us to treat each charge defect separately.

The negative charge on the defect sites maintains the electronic skeleton of the lattice, compensating for the locally missing valence electron. It is distributed to a significant extent over the surrounding O atoms as additional negative charge, because the electron affinity U_{ea} of oxygen (0.14 MJ/mol) is higher than the U_{ea} value of both Al and Mg (∼0.04 MJ/mol).[6] In the case of tetrahedral defects by Si → Al substitution, the three O neighbors on the surface are nearer to the interlayer cations and have lower partial charges than the fourth, apical O atom (section 5.1). Therefore, we distribute the excess charge only over these three O neighbors on the surface. In the case of octahedral layer defects by Al → Mg substitution, all six O neighbors have the same distance to the adjacent interlayers and have similar charges (section 5.1). Therefore, we spread the excess charge evenly over all six O neighbors.

Given the partial charge of +1.1 for Si in the tetrahedral layer and the partial charge of +1.45 for Al in the octahedral layer, the same covalent contributions in the lattice are made with a partial charge of 0.1 for a Si → Al defect and with a partial charge of 0.45 for a Al → Mg defect, respectively.[61] In these cases, the partial charges on the neighboring O atoms would remain the same as those without substitution. However, the electrostatic energy in the defects, which is proportional to the partial charge, would be substantially reduced, compared to a nondefective lattice. Thus, the defect metals are ionized to a higher degree so that a balance between the ionic contribution and the covalent contribution is established. The charge of the affected bonded O atoms is then larger than that in a nondefective lattice.

Because of the slight decrease of $\Delta H_{at} + \Delta U_i^I$ from Si to Al, the maximum charge for Al-defects is +1.3 instead of +1.1 for Si (see argument (7) in section 5.1). Similarly, the sum of the atomization energy and the first two ionization energies ($\Delta H_{at} + \Delta U_i^I + \Delta U_i^{II}$) decreases from Al to Mg (see Table 3) and the maximum charge for Mg-defects will be +1.6 instead of +1.45. In the case of these maximum charges, however, the charge difference of ∼1.2 toward optimum covalent bonding weakens the framework of localized bonds substantially and causes excessive additional negative charges on the neighboring O atoms, which is unfavorable.

Balancing the covalent and ionic contributions yields atomic charges of +0.8 (±0.2) for Al-defects and +1.1 (±0.2) for Mg-defects. We presume, with these charges, that the influence of the electrostatic energy is slightly higher than that of the covalent contribution. The charge of the three O neighbors of Al-defects is then $-0.55 - (0.8 - 0.1)/3 = -0.78333$. Similarly, the charge of the six O atoms connected to Mg-defects is −0.86666 when connected to the tetrahedral layer and −0.79166 when part of a hydroxyl group.

The complete atom-based charges for mica and montmorillonite are summarized in Table 8. Muscovite mica usually has

no Mg-defects in the octahedral layer, and montmorillonite usually has no Al-defects in the tetrahedral layer, in agreement with the formulas.

5.3. Charges in Tetraalkylammonium Ions. Tetraalkylammonium ions are common surfactants that are used to change the polarity of mineral surfaces.[11,13,15] Strongly negative nitrogen charges, such as -0.63[9] or other negative values in excess of -0.4 from theoretical methods indicated in Table 2, are in use. This seems surprising, because this class of ions has an overall positive charge of $+1$. The dipole moment[6] of neutral trimethylamine ($N(CH_3)_3$) yields a partial charge of only -0.28 on the nitrogen and $q_c = +0.093$ on each C atom.[62] The charge on the N atom would be even closer to zero when we extend the dipole length by spreading some positive charge over the H atoms.

To construct a tetraalkylammonium cation, we attach a positively charged carbocation to the nitrogen of $N(CH_3)_3$. The incoming positive charge from the carbocation spreads over the N atom and the three C atoms of $N(CH_3)_3$, such that all four C atoms ultimately have the same charge. Assuming that the N atom and the three C atoms with a initial charge q_c in $N(CH_3)_3$ take up the same partial charge x from the added carbocation, we obtain, for the final carbon charge, $q_{c'} = q_c + x = 1 - 4x$. The result is a charge of $q_{c'} = +0.275$ on the C atom and a charge of -0.10 on the N atom in the tetraalkylammonium ion. Nitrogen may actually transfer slightly more or less electron density than the three C atoms of $N(CH_3)_3$ to the incoming carbocation. However, our result probably suffers a deviation of no more than ± 0.1 for N (see Table 8).

6. Evaluation

We have now introduced our semiempirical model of polar bonding and demonstrated that errors in theoretically derived charges can be reduced from more than ± 1.0 e to ± 0.2 e, which is practically consistent with experimentally determined charges. However, it is also important to assess the improvement of simulations with our charge estimates. The following examples demonstrate the main advances (an extensive validation would exceed the scope of this article).

Potential models for common molecules have been iterated many times to achieve optimum parametrizations. The resulting atomic charges usually coincide closely with experimental values, which we have discussed in detail for water and formaldehyde in section 2.2. Only the charges similar to those of the experiment allow for a good reproduction of coordination geometries, distribution functions, phase diagrams, and interaction energies.[44−46] Our concept generally suggests such values, including those for water and formaldehyde (see sections 4 and 5.1).

We extended the polymer consistent force field to several minerals: mica,[15] montmorillonite,[63] and other industrially important silicates and aluminates.[64] Unit-cell parameters (a, b, c, α, β, γ) in earlier mineral models with different charges are usually reproduced with an error on the order of 5%, compared to published crystal structures.[12a,37,38,48,65] Often, it was difficult to make stable models without significant distortions or other artifacts.[8,9,37] In all our models, the unit-cell parameters are reproduced with an error on the order of only 0.5%, compared to published crystal structures, using less than 10 force-field types.[15,63,64] Thus, the reproduction of crystal structures is an order of magnitude more accurate. In simulations of inorganic−organic interfaces, rearrangements of amphiphilic ions on the mica surface, as a function of temperature, have been observed in good agreement with differential scanning calorimetry (DSC), infrared (IR), NMR, and X-ray data.[15] Simulated X-ray patterns (e.g., for surface-modified montmorillonite[63]) match those of the experiments, in regard to all major and minor peaks. In addition, adsorption energies of polyelectrolytes and single ions have been obtained in (at least) semiquantitative agreement with the experiment on different silicate and aluminate surfaces.[64]

Herzbach, Muser, and Binder recently investigated the entire phase diagram of SiO_2 with different force fields.[66] The BKS model with a Si charge of $+2.4$[36] shows significantly more deviations in the reproduction of X-ray data and phase coexistence lines than two models, based on a principal Si charge of $+1.2$ with fluctuations.[66] The Si charge of $+1.2$ is within the range of our estimate ($+1.1$; see Table 8) and clearly better suited.

Individual charges have been sometimes empirically set to values, which improve the reproduction of crystal structures and interfacial phenomena.[10a,10c,10d,14a,42,67] Although some of these charges are similar to our results, others are not: e.g., $+1.2$ for Si but $+3$ for Al,[10a,10c,10d,14a] or $+1.6$ for Al but $+2.1$ for Si.[67] This leads to an inconsistency in Coulomb energies, which has no experimental or theoretical justification. Nevertheless, these partly accurate charges improve somewhat the performance compared to force fields with more arbitrary values (deviations in unit-cell parameters of $\sim$2%).

We summarize that, according to our examples, atomic charges that are similar to the experimental values are best-suited in semiempirical simulations and values according to the extended Born model reduce common errors in structural reproduction up to 1 order of magnitude, as well as discrepancies in phase diagrams. More-reliable interface structures and energies can be obtained.

7. Conclusions

We introduce a semiempirical model to understand the polarity of compounds, based on properties of the constituting elements that characterize the capability for covalent and ionic bonding. The atomization energies of the elements correlate with the tendency of covalent bonding and the ionization energies/electron affinities of the elements determine the extent of ionic bonding. In addition, higher polarizability (related to the sum of ionization energy and ionization energy) strengthens the tendency for covalent bonding. The two main contributions are approximately equally important, in regard to estimating the polarity. The relationship between these quantities for elements and a compound is shown in an extended Born model, which explicitly considers covalent and ionic bonding contributions to the cohesive energy.

For semiempirical estimates of partial charges, the atomization energies and ionization potentials/electron affinities of the constituting elements can be evaluated, relative to reference compounds with experimentally determined charges. Following this concept and basic chemical and physical knowledge, atomic charges with an uncertainty of ± 0.1 e to ± 0.3 e can be obtained. For example, we discussed charges in several alkali, alkali-earth, aluminum, and zinc halides and paid particular attention to SiO_2, mica, montmorillonite, local charge defects, and alkylammonium ions. Force fields based on these charges for several minerals accurately reproduce crystal structures (geometric deviations of $\sim$0.5% in unit-cell parameters with less than 10 force-field types), reduce errors in phase diagrams, and yield physically more-realistic interfacial structures and energies.

In principle, the extended Born model provides an exact understanding of the polarity in chemical bonding. However, it

is difficult to quantify the ionization potentials and electron affinities for fractional charges, as well as the contributions to the cohesive energy, exactly. This poses a challenge for experiments and first-principle approaches. Currently, the semiempirical approach, relative to reference compounds and physical-chemical data, is more convenient and precise; quantum-chemical methods cannot (yet) predict charges sufficiently well.

Acknowledgment. We express our thanks to Epameinondas Leontidis (Department of Chemistry, University of Cyprus) for helpful discussions. The support from the Swiss Federal Institute of Technology (ETH Zürich), the Swiss National Science Foundation (Schweizerischer Nationalfonds), and the German National Merit Foundation (Studienstiftung des Deutschen Volkes) is acknowledged.

References and Notes

(1) (a) Catlow, C. R. A., Parker, S. C., Allen, M. P., Eds. *Computer Modelling of Fluids, Polymers, and Solids*; Kluwer: Dordrecht, The Netherlands, 1990. (b) Allen, M. P., Tildesley, D. J., Eds. *Computer Simulation in Chemical Physics*; Kluwer: Dordrecht, The Netherlands, 1993. (c) Allen, M. P.; Tildesley, D. J. *Computer Simulation of Liquids*; Clarendon Press: Oxford, U.K., 2000.

(2) Höltje, H.-D.; Sippl, W.; Rognan, D.; Folkers, G. *Molecular Modeling. Basic Principles and Applications*, 2nd Edition; Wiley−VCH: Weinheim, Germany, 2003.

(3) Born, M. *Verh. Dtsch. Phys. Ges.* **1919**, *21*, 13−24.

(4) Haber, F. *Verh. Dtsch. Phys. Ges.* **1919**, *21*, 750−768.

(5) Tosi, M. P. *Solid State Phys.* **1964**, *16*, 1−120.

(6) Lide, D. R., Ed. *CRC Handbook of Chemistry and Physics*, 83th Edition; CRC Press: Boca Raton, FL, 2002.

(7) (a) Rothbauer, R. *N. Jahrb. Mineral. Monatsh.* **1971**, 143−154. (b) Vogt, K.; Köster, H. M. *Clay Miner.* **1978**, *13*, 25−43. (c) Jasmund, K., Lagaly, G., Eds. *Tonminerale und Tone*; Steinkopff: Darmstadt, Germany, 1993. Typical compositions for the minerals are given.

(8) Hill, J. R.; Sauer, J. *J. Phys. Chem.* **1995**, *99*, 9536−9550.

(9) Teppen, B. J.; Rasmussen, K.; Bertsch, P. M.; Miller, D. M.; Schäfer, L. *J. Phys. Chem. B* **1997**, *101*, 1579−1587.

(10) (a) Boek, E. S.; Coveney, P. V.; Skipper, N. T. *J. Am. Chem. Soc.* **1995**, *117*, 12608−12617. (b) Liang, J.-J.; Hawthorne, F. C. *Can. Mineral.* **1998**, *36*, 1577−1585. (c) Greathouse, J. A.; Refson, K.; Sposito, G. *J. Am. Chem. Soc.* **2000**, *122*, 11459−11464. (d) Young, D. A.; Smith, D. E. *J. Phys. Chem. B* **2000**, *104*, 9163−9170.

(11) Manne, S.; Gaub, H. E. *Science* **1995**, *270*, 1480−1482.

(12) (a) Karaborni, S.; Smit, B.; Heidug, W.; Urai, J.; van Oort, E. *Science* **1996**, *271*, 1102−1104. (b) Liley, M.; Gourdon, D.; Stamou, D.; Meseth, U.; Fischer, T. M.; Lautz, C.; Stahlberg, H.; Vogel, H.; Burnham, N. A.; Duschl, C. *Science* **1998**, *280*, 273−275.

(13) Osman, M. A.; Ernst, M.; Meier, B. H.; Suter, U. W. *J. Phys. Chem. B* **2002**, *106*, 653−662.

(14) (a) Kuppa, V.; Manias, E. *Chem. Mater.* **2002**, *14*, 2171−2175. (b) Yu, K.-Q.; Li, Z.-S.; Sun, J.-Z. *Langmuir* **2002**, *18*, 1419−1425.

(15) (a) Heinz, H.; Castelijns, H. J.; Suter, U. W. *J. Am. Chem. Soc.* **2003**, *125*, 9500−9510. (b) Heinz, H.; Paul, W.; Suter, U. W.; Binder, K. *J. Chem. Phys.* **2004**, *120*, 3847−3854. (c) Heinz, H.; Suter, U. W. *Angew. Chem., Int. Ed.* **2004**, *43*, 2239−2243.

(16) Brill, R.; Hermann, C.; Peters, C. *Z. Anorg. Allg. Chem.* **1948**, *257*, 151−165.

(17) Witte, H.; Wölfel, E. *Rev. Mod. Phys.* **1958**, *30*, 51−55.

(18) Aref'ev, K. P.; Vorob'ev, S. A. *Izv. Vyssh. Uchebn. Zaved., Fiz.* **1972**, *15*, 34−38.

(19) Hill, R. J. *Phys. Chem. Miner.* **1979**, *5*, 179−200.

(20) Göttlicher, S.; Knöchel, C. D. *Acta Crystallogr., Sect. B: Struct. Crystallogr. Cryst. Chem.* **1980**, *B36*, 1271−1277.

(21) Ngo, T.; Schwarzenbach, D. *Acta Crystallogr., Sect. A: Cryst. Phys., Diffr., Theor., Gen. Crystallogr.* **1979**, *A35*, 658−664.

(22) Lewis, J.; Schwarzenbach, D. *Acta Crystallogr., Sect. A: Cryst. Phys., Diffr., Theor., Gen. Crystallogr.* **1982**, *A38*, 733−739.

(23) Wood, J. S. *Inorg. Chim. Acta* **1995**, *229*, 407−415.

(24) Belokonewa, E. L.; Gubina, Yu. K.; Forsyth, J. B.; Brown, P. J. *J. Phys. Chem. Min.* **2002**, *29*, 430−438.

(25) Greenwood, N. N.; Earnshaw, A. *Chemistry of the Elements*; Pergamon Press: Oxford, U.K., 1984.

(26) Bachrach, S. M. *Rev. Comput. Chem.* **1994**, *5*, 171−227.

(27) Rappé, A. K.; Goddard, W. A., III. *J. Phys. Chem.* **1991**, *95*, 3358−3363.

(28) (a) Hoffmann, R. *J. Chem. Phys.* **1963**, *39*, 1397−1412. (b) Zhang, X.; Li, J.; Foran, B.; Lee, S.; Guo, H. Y.; Hogan, T.; Kannewurf, C. R.; Kanatzids, M. G. *J. Am. Chem. Soc.* **1995**, *117*, 10513−10520.

(29) Mulliken, R. S. *J. Chem. Phys.* **1955**, *23*, 1833−1840.

(30) Politzer, P.; Mulliken, R. S. *J. Chem. Phys.* **1971**, *55*, 5135−5136.

(31) Bader, R. F. W.; MacDougall, P. J.; Lau, C. D. H. *J. Am. Chem. Soc.* **1984**, *106*, 1594−1605.

(32) Bader, R. F. W.; MacDougall, P. J. *J. Am. Chem. Soc.* **1985**, *107*, 6788−6795.

(33) Chirlian, L. E.; Francl, M. M. *J. Comput. Chem.* **1987**, *8*, 894−905.

(34) Cioslowski, J. *Phys. Rev. Lett.* **1989**, *62*, 1469−1471.

(35) Cioslowski, J. *J. Am. Chem. Soc.* **1989**, *111*, 8333−8336.

(36) Van Beest, B. W. H.; Kramer, G. J.; Van Santen, R. A. *Phys. Rev. Lett.* **1990**, *64*, 1955−1958.

(37) Hill, J.-R.; Sauer, J. *J. Phys. Chem.* **1994**, *98*, 1238−1244.

(38) Teppen, B. J.; Miller, D. M.; Newton, S. Q.; Schäfer, L. *J. Phys. Chem.* **1994**, *98*, 12545−12557.

(39) Francl, M. M.; Carey, C.; Chirlian, L. E.; Gange, D. M. *J. Comput. Chem.* **1996**, *17*, 367−383.

(40) Delley, B. *J. Chem. Phys.* **1990**, *92*, 508−517.

(41) Terra, J.; Ellis, D. E. *Phys. Rev. B* **1997**, *56*, 1834−1847.

(42) Kalinichev, A. G.; Kirkpatrick, R. J.; Cygan, R. T. *Am. Mineral.* **2000**, *85*, 1046−1052.

(43) For water, the dipole moment is given by the H−O−H angle α and the O−H distance d, according to the relation $|\vec{\mu}| = 2q_H ed \cos \alpha/2$, where e is the elementary charge.

(44) Mahoney, M. W.; Jorgensen, W. L. *J. Chem. Phys.* **2000**, *112*, 8910−8922. The oxygen charge in this model is distributed over the two lone pairs. The equivalent atom-based charge for the O atom would be slightly higher than the sum of the two lone-pair charges because it would be placed nearer to the H atom.

(45) Jorgensen, W. L. *J. Am. Chem. Soc.* **1981**, *103*, 335−340.

(46) *Cerius*^{2} *and Discover Program*; Molecular Simulations, Inc.: San Diego, CA, 1996.

(47) Abbott, R. N., Jr.; Post, J. E.; Burnham, C. W. *Am. Mineral.* **1989**, *74*, 141−150.

(48) Collins, D. R.; Catlow, C. R. A. *Am. Mineral.* **1992**, *77*, 1172−1181.

(49) Pauling, L. *The Nature of the Chemical Bond*; Cornell University Press: Ithaca, NY, 1960.

(50) Pauling, L. *Am. Mineral.* **1980**, *65*, 321−323.

(51) Gibbs, G. V.; Downs, J. W.; Boisen, M. B., Jr. *Rev. Mineral.* **1994**, *29*, 331−368.

(52) Horbach, J.; Kob, W.; Binder, K. *Phys. Rev. Lett.* **2002**, *88*, 125502.

(53) Huheey, J. E.; Keiter, E. A.; Keiter, R. L. *Inorganic Chemistry. Principles of Structure and Reactivity*, 4th Edition; Harper Collins: New York, 1993.

(54) (a) Parr, R. G.; Pearson, R. G. *J. Am. Chem. Soc.* **1983**, *105*, 7512−7516. (b) Mortier, W. J.; Ghosh, S. K.; Shankar, S. *J. Am. Chem. Soc.* **1986**, *108*, 4315−4320.

(55) The Born model is sometimes called the Born−Haber cycle or the Born−Haber−Fajans cycle.

(56) The difference between the enthalpies ΔH and energies ΔE is the expansion work $W = p^\circ V_m \approx RT^\circ \approx 3$ kJ/mol, where p° and T° are standard pressure and temperature, V_m is the molar volume of a gas, and R is the universal gas constant. W is significantly smaller than the atomization energies, ionization energies, electron affinities, or cohesive energies (see Tables 3 and 4), so the difference between ΔH and ΔE can be neglected.

(57) (a) Huttner, G.; Lorenz, H.; Gartzke, W.; Fischer, E. O. *Angew. Chem. Int. Ed.* **1974**, *13*, 609−611. (b) Pu, L. H.; Twamley, B.; Haubrich, S. T.; Olmstead, M. M.; Mork, B. V.; Simons, R. S.; Power, P. P. *J. Am. Chem. Soc.* **2000**, *122*, 650−656.

(58) Sometimes we need estimates of U_i or U_{ea} for fractional charges such as ± 0.5. For N, O, P, and S atoms, there is evidence for a maximum of the electron affinity for small negative charges, e.g., for -0.5 the Oelectron affinity is $\sim$0.14 MJ/mol (section 4.2). The U_{ea} value for fractional charges of halogens may be approximated by linear interpolation.

(59) The argument can be rendered more carefully if we examine the crystal structures in detail.

(60) (a) Sanz, J.; Serratosa, J. M. *J. Am. Chem. Soc.* **1984**, *106*, 4790−4793. (b) Lipsicas, M.; Raythatha, R. H.; Pinnavaia, T. J.; Johnson, I. D.; Giese, R. F.; Constanzo, P. M.; Robert, J. L. *Nature* **1984**, *309*, 604−607.

(61) Ionization from the initial charge of -1 to ± 0 requires less than the negligible amount of 0.05 MJ/mol for both Al and Mg (see refs 6 and

53). It is therefore sufficient to consider ionization from electroneutrality onward.

(62) The dipole moment of $N(CH_3)_3$ is given by the C−N−C angle α and the C−N distance d as $|\vec{\mu}| = \sqrt{3}q_c e d\sqrt{1+2\cos\alpha}$, according to elementary geometry.

(63) Heinz, H.; Koerner, H.; Farmer, B. L., to be published.

(64) Unpublished work.

(65) Manevitch, O. L.; Rutledge, G. C. *J. Phys. Chem. B* **2004**, *108*, 1428−1435.

(66) Herzbach, D. *Comparison of Model Potentials for Molecular Dynamics Simulation of Crystalline Silica*, Dissertation, Universität Mainz, Germany, 2004.

(67) Kalinichev, A. G.; Kirkpatrick, R. J. *Chem. Mater.* **2002**, *14*, 3539−3549.